






## Multi-objective topology optimisation for acoustic porous materials using gradient-based, gradient-free, and hybrid strategies

Vivek T. Ramamoorthy,<sup>1,a)</sup>  Ender Özcan,<sup>1</sup>  Andrew J. Parkes,<sup>1</sup>  Luc Jaouen,<sup>2</sup>   
 and François-Xavier Bécot<sup>2</sup> 

<sup>1</sup>Computational Optimisation and Learning Laboratory, School of Computer Science, University of Nottingham, NG8 1BB, United Kingdom

<sup>2</sup>Matelys-Research Laboratory, 7 Rue des Maraîchers, Vaulx-en-Velin, 69120, France

### ABSTRACT:

When designing passive sound-attenuation structures, one of the challenging problems that arise is optimally distributing acoustic porous materials within a design region so as to maximise sound absorption while minimising material usage. To identify efficient optimisation strategies for this multi-objective problem, several gradient, non-gradient, and hybrid topology optimisation strategies are compared. For gradient approaches, the solid-isotropic-material-with-penalisation method and a gradient-based constructive heuristic are considered. For gradient-free approaches, hill climbing with a weighted-sum scalarisation and a non-dominated sorting genetic algorithm-II are considered. Optimisation trials are conducted on seven benchmark problems involving rectangular design domains in impedance tubes subject to normal-incidence sound loads. The results indicate that while gradient methods can provide quick convergence with high-quality solutions, often gradient-free strategies are able to find improvements in specific regions of the Pareto front. Two hybrid approaches are proposed, combining a gradient method for initiation and a non-gradient method for local improvements. An effective Pareto-slope-based weighted-sum hill climbing is introduced for local improvement. Results reveal that for a given computational budget, the hybrid methods can consistently outperform the parent gradient or non-gradient method.

© 2023 Author(s). All article content, except where otherwise noted, is licensed under a Creative Commons Attribution (CC BY) license (<http://creativecommons.org/licenses/by/4.0/>). <https://doi.org/10.1121/10.0019455>

(Received 21 July 2022; revised 1 May 2023; accepted 2 May 2023; published online 19 May 2023)

[Editor: Kirill V. Horoshenkov]

Pages: 2945–2955

### I. INTRODUCTION

Acoustic porous materials, such as foams or fibrous materials, are widely used for passive noise control in automotive, aerospace, and construction industries. While these materials generally exhibit sound absorption across wide frequency bands, their low-frequency absorption performance is poor because the lengths of the absorber typically needed are higher for longer wavelengths.<sup>1</sup> To alleviate this problem, one can modify the absorber shape or introduce macro-scale air cavities<sup>2</sup> to alter the dynamic properties, creating favourable resonances that improve absorption while also reducing the material usage. It is known that by creating tortuous pathways with longer lengths than the dimension of the material, it is possible to improve low-frequency sound absorption. Exploring such shapes and solutions requires allowing material variations along other directions in addition to the primary direction of propagation. However, optimising the size, shape, and placement of these air cavities or other solid scattering materials<sup>3</sup> is essentially a topology optimisation problem,<sup>4</sup> which is challenging to solve.

Structural topology optimisation is the concept of simultaneously optimising the topology (number of holes in a structure) and shape (geometry and dimensions of these holes) of mechanical structures so as to maximise the load-bearing capacity with minimal material usage. It is a concept first introduced by Bendsøe and Kikuchi<sup>5,6</sup> in the 1990s and has remarkable potential benefits in terms of reduced weight and costs. In the last two decades, topology optimisation techniques have been extended to automatic generation of optimised acoustic shape designs in various applications, such as horns,<sup>7</sup> room sound treatments,<sup>8</sup> anechoic chamber foams,<sup>2,9</sup> mufflers,<sup>10–13</sup> sound barriers,<sup>14–17</sup> and car internal cavity,<sup>18</sup> to name a few. Although topology optimisation is inherently a multi-objective problem, i.e., simultaneously maximising performance and minimising weight, it has been common to treat it as a single-objective problem, i.e., maximising the performance while using a constraint on the weight. Given that one of the main potential benefits is the weight savings, it is of interest to treat it as a multi-objective problem and obtain multiple trade-off designs simultaneously. Acoustic designers can then choose from the set of Pareto optimal or trade-off solutions for manufacture.

While new and improved optimisation strategies are being published for particular applications, there is a need

<sup>a)</sup>Electronic mail: vivek.thaminniramamoorthy@nottingham.ac.uk

for comparison studies which would facilitate the acoustic designers to choose the most effective strategy for their use case. Performing such comparisons is challenging as many optimisation paradigms are available for topology optimisation problems that vary in solution representation (discrete or continuous), gradient usage, memory (single-point or population-based), move operators, acceptance strategies, etc., and to ensure a fair comparison among different strategies, each algorithm needs to be applied in the best or most reasonable settings tuned to the problem domain. The goal of this article is to identify effective multi-objective topology optimisation algorithms for acoustic shape design. To achieve this, a few selected approaches that are popular and likely to be used by other researchers are compared. The approaches chosen are as follows:

- Solid isotropic material with penalisation (SIMP);
- constructive heuristic with gradient (CHg);
- hill climbing with weighted-sum scalarisation (HC); and
- non-dominated sorting genetic algorithm-II (NSGA-II).

SIMP is a gradient-based approach for structural topology optimisation.<sup>19–21</sup> A key attribute of this approach is the relaxation of the discrete problem of choosing between the presence or absence of material at each finite element in the design domain into a continuous problem by allowing intermediate materials in each element and using a power-law interpolation scheme to represent the material properties for the intermediate materials. By allowing such fictitious intermediate materials, it becomes possible to quickly compute the sensitivity of structural performance to the interpolation design variable, and the optimisation can be performed faster. Despite certain drawbacks, such as needing to re-derive the gradient equations for each application or the algorithm getting stuck at local-optimal solutions, the effectiveness and ease of implementation of SIMP<sup>22</sup> have made it the most popular approach for topology optimisation. At this point, it is worth noting some previous efforts toward extending SIMP for multi-objective topology optimisation. Suresh *et al.*<sup>23</sup> studied the effects of restarts vs hot starts for effective Pareto optimal compliance minimisation. In restart SIMP, the algorithm is run from uniform-density or random initial solutions with different volume fraction constraints. Whereas in hot starts, the optimised solution obtained from a previous run of SIMP is reused as an initial solution in the next run. Such studies have not been conducted for absorption maximisation. Hence, in this study, two variants, SIMPsweep and SIMPrestart, are considered. Mirzendehtel and Suresh<sup>24</sup> proposed a multi-objective algorithm for multi-material compliance minimisation, removing the mass constraint and treating it as an objective. Fu<sup>25</sup> presented an account on the advances in multi-objective topology optimisation, including NSGA-II and weighted-sum scalarisation. Although the multi-objective consideration is prevalent, it constitutes a small fraction of the publications, and comparison studies are rare.

Constructive heuristics are a class of optimisation algorithms that start from empty solutions and build them step

by step using specific move operations to reach a complete solution. An example of a constructive heuristic for topology optimisation is the (bidirectional) evolutionary structural optimisation methods (ESO/BESO) introduced by Xie and Steven.<sup>26,27</sup> For compliance minimisation, ESO starts from a completely solid-filled design domain and incrementally removes material from low-stress regions. For acoustic material topology optimisation, Ramamoorthy *et al.*<sup>9</sup> introduced two constructive heuristics: CH1, where the material is added incrementally to an empty domain in places of highest absorption increase; and CH2, where the material is incrementally removed from a filled domain from places where the decrease in absorption is minimal. These heuristics performed among the top strategies in the study. One of the drawbacks of CH1 and CH2 is that computing the numerical absorption increments is expensive, and this can be overcome by making use of the gradients. Adopting this, a simple gradient-based constructive heuristic (CHg) is proposed in the current study.

Hill climbing is a single-objective optimisation technique that starts with an initial solution and modifies it iteratively while accepting improving changes. A row-wise hill climbing approach was found to perform among the best strategies for acoustic material absorption maximisation.<sup>9</sup> A common strategy to solve multi-objective problems is to combine the objectives into a scalar value in a process known as scalarisation<sup>25,28</sup> and apply a single-objective algorithm. A simple way to scalarise is to use the weighted sum of the objectives. By varying the weights, the relative importance of each objective can be controlled. In this study, hill climbing is used in conjunction with a weighted-sum scalarisation technique (HC) as a candidate for multi-objective topology optimisation.

NSGA-II, introduced by Deb *et al.*,<sup>29</sup> is a widely used multi-objective evolutionary algorithm. A notable attribute of NSGA-II is the use of a fast non-dominated sorting procedure in combination with a crowding-distance operator that allows finding multiple points in the Pareto front simultaneously, as opposed to having to run multiple trials of a single-objective algorithm in combination with a scalarisation technique. The effectiveness of NSGA-II and its variants has made it the most popular multi-objective approach for solving combinatorial optimisation problems.<sup>30</sup>

In addition to the above strategies, hybrid approaches 1 and 2 (HA1 and HA2) are proposed, involving a gradient method for initialisation and a non-gradient method for local improvement. The aim is to identify whether hybridising approaches are beneficial. The results will provide perspectives on each method and guide algorithm selection for acoustic designers.

To test the above optimisation approaches, a finite element-based poroelastic model is used to describe the materials, a set of seven benchmark problems involving rectangular impedance tube systems with varying dimensions and materials are considered, and the optimisation of the shapes are performed at wide frequency bands. A fixed computational budget is allowed for all of the methods, and

a hypervolume metric is used to assess the Pareto fronts obtained from each algorithm.

The article is organised as follows. In Sec. II, the overall methodology, including problem description, optimisation formulation, modelling method, and the design of experiments for optimisation methods, is provided. In Sec. III, a comparison of gradient algorithms—SIMP sweep, SIMP start, and CHg is provided. In Sec. IV, a comparison of gradient-free algorithms, HC and NSGA-II, are provided. Along with gradient-free algorithms, a random search procedure is also compared. In Sec. V, two hybrid approaches, HA1 and HA2, are described and compared with their parent approaches. Finally, in Sec. VI, a summary of the findings and some general guidelines to design algorithms are provided.

## II. METHODOLOGY

### A. Problem formulation

Consider the problem of optimally filling a rectangular design domain as shown in Fig. 1(a) with a given porous material such that the sound absorption is maximised while minimising the material used. The design domain can be assumed to be backed by rigid walls subject to a normal-incidence acoustic source. Sound absorption is the ratio of energy absorbed to the total input sound energy. If no porous material is placed in the design domain, there would not be any absorption. Typically, as more porous material is filled in the design domain, the absorption would increase, but this is not always the case. There are instances when removing material would improve absorption.<sup>9</sup> Depending on the distribution of porous material and air in the design domain, sound absorption will be determined at different frequencies of the acoustic source. Thus, this is a classic bi-objective optimisation problem with trade-off solutions.

While there are many ways to formulate the topology optimisation problem, one of the classical ways is to use a fixed finite element discretisation of the system and optimise the material assigned to each finite element. The shape and topology can be represented by a vector,  $\chi$ , with zeros and ones corresponding to the absence or presence of porous material in each element, respectively, as shown in Fig. 1(b). This is sometimes referred to as a bit-matrix representation.<sup>31</sup>

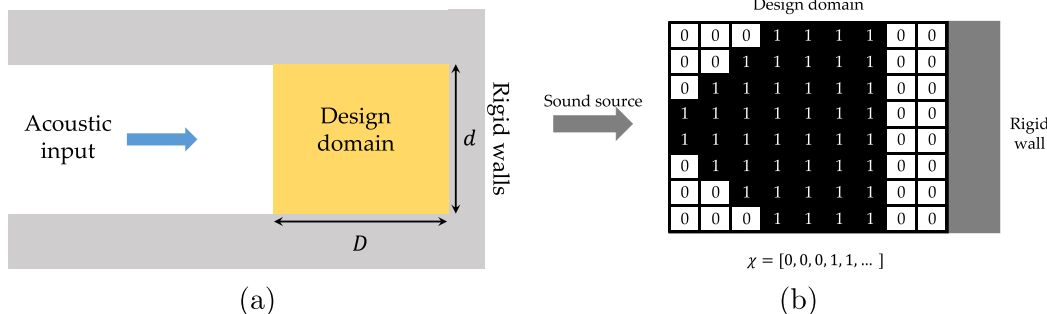


FIG. 1. (Color online) (a) Schematic of an acoustic system with the design domain and (b) binary representation of a sample shape are shown. Zeros refer to air and ones refer to the base porous material.

At this point, it is also worth acknowledging other formulations such as moving morphable components,<sup>32</sup> level-set method,<sup>33,34</sup> etc. The objective considered is to find the optimal discrete assignments of either air or a given poroelastic material to each finite element that simultaneously maximises the normal sound absorption and minimises the volume fraction of the porous material. Mathematically, this formulation can be written as

$$\max_{\chi} \quad \bar{\alpha}(\chi) = \frac{1}{n_f} \sum_{i=1}^{n_f} \alpha(\chi, f_i), \tag{1}$$

$$\min_{\chi} \quad V_f(\chi) = \frac{1}{n_e} \sum_{i=1}^{n_e} \chi_i, \tag{2}$$

$$\chi \in \{0, 1\}^{n_e},$$

$$\bar{\alpha} \in [0, 1],$$

$$V_f \in [0, 1].$$

The first objective,  $\bar{\alpha} \in [0, 1]$ , is the sound absorption averaged across the target frequencies,  $(f_1, f_2, \dots, f_{n_f})$ , and the second objective,  $V_f$ , is the porous volume fraction. Absorption,  $\bar{\alpha}$ , is averaged over a number of target frequencies,  $n_f$ , and porous material volume fraction,  $V_f$ , is averaged over the number of elements,  $n_e$ , in the design domain. Normal-incidence sound absorption is used to reduce the computational time for the tests. The results may be extended to diffused field sound absorption, which is more appropriate for practical purposes.

### B. Computing the objectives

Computing the volume fraction  $V_f$  for a given shape,  $\chi$ , is quick and straightforward from Eq. (2), whereas computing absorption  $\bar{\alpha}$  is time-consuming, requiring solving a finite element model of the acoustic system. To compute  $\bar{\alpha}$ , we model the acoustic system using a unified Biot-Helmholtz model introduced by Lee *et al.*,<sup>2</sup> which considers all of the materials to be poroelastic. Such modelling avoids treating interfaces explicitly and simplifies the numerical procedure. In this method, for intermediate materials between air and poroelastics, i.e.,  $\chi_i \in (0, 1)$ , the material parameters are interpolated using a power-law, i.e., a material parameter, say,  $\psi_i$  is given by  $\psi_{\text{air}} + \chi_i^p (\psi_{\text{por}} - \psi_{\text{air}})$ ,

where  $\psi_{\text{por}}$  and  $\psi_{\text{air}}$  are the parameters of the porous material and air, respectively. To avoid numerical issues when solving the system, air is modelled as a poroelastic material with a negligible solid-phase behaviour, i.e.,  $\chi_{\text{air}} = 0.001$ . Lee *et al.*<sup>2</sup> have also verified the validity of such a procedure with explicit interface modelling for various shapes. The unified poroelastic system is then modelled using mixed formulations by Atalla *et al.*,<sup>35</sup> and the system equations are written in matrix form as  $[\tilde{\mathbf{S}}(\boldsymbol{\chi}, f)] \begin{Bmatrix} \tilde{\mathbf{u}} \\ \tilde{\mathbf{p}} \end{Bmatrix} = \{\tilde{\mathbf{F}}\}$ . Here,  $[\tilde{\mathbf{S}}(\boldsymbol{\chi}, f)]$  is the dynamic stiffness matrix, which depends on the material assignments,  $\boldsymbol{\chi}$ , and the frequency-dependent material parameters.  $\tilde{\mathbf{u}}$  and  $\tilde{\mathbf{p}}$  correspond to the nodal solution to the solid-phase displacements and fluid acoustic pressures, respectively. By solving the linear system, pressure and velocity fields are found and sound absorption can be computed at the target frequencies using the two-microphone method.

The gradient of sound absorption with respect to the topological design variables is computed by progressively applying the chain rule in differentiation on the absorption computation. For further details, one may refer to Ramamoorthy *et al.*<sup>9</sup> Once the linear system is solved to compute  $\bar{\alpha}$ , the gradient,  $\partial\bar{\alpha}/\partial\boldsymbol{\chi}$ , can be computed in approximately two additional instances of solving the system of linear equations, making gradient algorithm fitness evaluations thrice as expensive as computing absorption.

$$\text{Time to compute } \bar{\alpha} \text{ and } \frac{\partial\bar{\alpha}}{\partial\boldsymbol{\chi}} \approx 3 \times \text{time to compute } \bar{\alpha}. \quad (3)$$

Such a quick computation of the gradient is achieved using a fictitious load vector pre-multiplication, as explained in Lee *et al.*<sup>12</sup> Thus, computing absorption and the gradient is three times as expensive as computing just absorption. Therefore, the gradient methods will be given one-third of the fitness evaluation budget. Fitness evaluation corresponds to the number of times  $\bar{\alpha}$  and  $V_f$  are evaluated.

### C. Benchmark problem instances

To compare the optimisation approaches, seven benchmark problem instances, which were previously introduced in Ramamoorthy *et al.*,<sup>9</sup> are adopted. The only difference here is that a modification has been made in the mesh size in problem instance 3 to improve the model accuracy. For completeness, the details of the problem instances are provided in Table I. The parameters in Table I, *nelx* and *nely*, are the number of finite elements horizontally and vertically across the design domain, *D* and *d* are the lengths and widths of the design domain, respectively,  $f_{\text{min}}$  and  $f_{\text{max}}$  are the lower and upper limits of the frequency, respectively, and  $f_{\text{step}}$  is the frequency increment. All of the problem instances have a rectangular design domain with varying dimensions, discretisation, the porous material filled, and frequency range of interest. Table II provides the poroelastic material properties for the materials used in the problem instances. While problem instance 1 uses the same material as was employed in Lee *et al.*<sup>2</sup> with a high tortuosity, the

TABLE I. Benchmark problems (see Sec. II C).

Problem Instance	Mesh size <i>nelx</i> × <i>nely</i>	Length <i>D</i> (m)	Height <i>d</i> (m)	$f_{\text{min}}$ (Hz)	$f_{\text{step}}$ (Hz)	$f_{\text{max}}$ (Hz)	Material identification (see Table II)
1	10 × 10	0.135	0.054	100	100	1500	(1)
2	15 × 10	0.045	0.1	100	100	1500	(2)
3	50 × 20	0.1	0.1	50	50	500	(3)
4	10 × 10	0.02	0.1	100	100	1500	(2)
5	10 × 10	0.02	0.1	2000	1000	5000	(2)
6	50 × 20	0.135	0.054	100	100	1500	(2)
7	10 × 5	0.135	0.054	500	500	500	(2)

third problem instance uses a fictitious material with high airflow resistivity, and all of the other problem instances use melamine. A Johnson-Champoux-Allard-Lafarge (JCAL) model (Refs. 36–38) was used to represent the acoustic material behaviour in these materials.

### D. Experimental design for optimisation trials

Table III provides a quick summary of the optimisation approaches used in this study along with a pseudocode of each approach. More detailed descriptions of each algorithm are provided in Secs. III–V. Reasonable effort has been made to use each algorithm in its recommended or best settings from parameter tuning and in the standard way unless otherwise stated.

All of the strategies were given the same arbitrarily chosen computational budget of 4096 equivalent gradient-free fitness evaluations. Gradient algorithms were assigned  $4096/3 \approx 1365$  fitness evaluations, and the non-gradient methods are allowed 4096 fitness evaluations. For the hybrid algorithms, 25% of the computational effort was allotted for gradient-based search and 75% was allotted for non-gradient search, i.e.,  $25\% \times 4096/3$  gradient-included and  $75\% \times 4096$  gradient-free fitness evaluations. Each non-gradient computation takes a fraction of a second to about 4 s, depending on the problem instance on a reference

TABLE II. Materials used in the benchmark problems and their properties (see Table I).

Material parameters	Material-1	Material-2	Material-3
Material	Lee <i>et al.</i> (Ref. 2)	Melamine	High-resistivity foam
Acoustic model	Johnson, Champoux, Allard, Lafarge (Refs. 36–38)	JCAL	JCAL
$\phi$	0.9	0.99	0.8
$\Lambda'$ ( $\mu\text{m}$ )	449	196	100
$\Lambda$ ( $\mu\text{m}$ )	225	98	10
$\sigma$ ( $\text{N s m}^{-4}$ )	25 000	10 000	300 000
$\alpha_{\infty}$	7.8	1.01	3
$k'_0$	4.75e-09	4.75e-09	4.75e-09
$\rho$ ( $\text{kg m}^{-3}$ )	31.08	8	80
$E$ (Pa)	800 000	160 000	30 000
$\nu$	0.4	0.44	0.44
$\eta$	0.265	0.1	0.01

TABLE III. Optimisation approaches and their settings.

Algorithm	Description and pseudocode	Deterministic or stochastic	Trials	Fitness evaluation budget per trial
Gradient-based approaches				
SIMPrestart	SIMP restarted with different volume fraction constraints $\hat{V}_f$ : A gradient-based strategy with optimality criteria move-update, following Ref. 39. Initialised with random solutions; restarted with a new $\hat{V}_f$ until budget is used up.	Stochastic: multiple restarts within trial	1 (many restarts)	1365 (with gradient)
SIMP sweep	SIMP with adaptive volume fraction constraint: Initialised with an empty design domain; volume fraction constraint, $\hat{V}_f$ , updated after each fitness evaluation reached one as budget approaches.	Deterministic	1	1365 (with gradient)
CHg	Gradient-based constructive heuristic: Start from an empty solution; add porous material in steps of “ $m$ ” elements, where the gradient is highest, until all elements are porous	Deterministic	1	$\min(n_e/m, 1365)$ (with gradient)
Non-gradient approaches				
HC	Hill climbing: Use a weighted-sum scalarisation technique to combine the two objectives into a single fitness value. Apply first improvement hill climbing starting from a random discrete solution. Move order is like in a raster-scan.	Stochastic, as initial solution is random	15	4096 (non-gradient)
NSGA-II	NSGA-II (Ref. 29): Use a bit representation, tournament selection based on crowding distance and rank, uniform crossover, bit-wise mutation probability of $1/N$ .	Stochastic	15	4096 (non-gradient)
RAND	Random search algorithm: Pick a desired volume fraction uniformly $\in [0, 1]$ ; use this as the probability of porous material at each element and synthesise a solution. Repeat budget number of times.	Stochastic	15	4096 (non-gradient)
Hybrid approaches				
HA1	Hybrid approach 1: Run CHg using 25% of the budget, and run hill climbing for 75% of the budget starting from a selected solution with scalarisation weight such that the combined objective isoline at the solution point in objective space is tangential to the Pareto front.	Deterministic but depends on the point picked for hill climbing	15	4096 (equivalent non-gradient)
HA2	Hybrid approach 2: Run CHg using 25% of the budget, and run NSGA-II for 75% of the budget starting from an initial population from equispaced points in the CHg Pareto front.	Stochastic	15	4096 (equivalent non-gradient)

computer. For the largest problem instance, this translates to a computational budget of about 4.5 h for 4096 fitness evaluations per trial and about 2.8 days for 15 trials of a method.

It should be noted that the resulting SIMP solutions had intermediate materials in some trials on some problem instances. In such scenarios, the non-dominated solutions were discretised by a round-off filter and the fitnesses were recomputed. This is performed so that all of the solutions compared in this study are from the discrete space to facilitate a fair comparison.

To quantify and compare the non-dominated solution set produced by each algorithm, a hypervolume metric is used. The hypervolume value corresponding to a given set of trade-off solutions is the scalar value equal to the union of volumes in the objective space dominated by each solution over the objective values of a given reference solution. An illustration is shown in Fig. 2. For the bi-objective problem under study, the hypervolume would simply be the area of the objective space that is dominated by the Pareto set obtained from the algorithms from a reference point. The reference point chosen is  $(\bar{\alpha}, V_f) = (0, 1)$ . A larger hypervolume of the Pareto solutions indicates a better performance of the multi-objective method.

### III. GRADIENT APPROACHES

#### A. SIMP

SIMP is a single-objective topology optimisation method, which uses volume fraction constraint,  $\hat{V}_f$ , as an input parameter. To use SIMP in the multi-objective context, two implementations, namely, SIMPrestart and SIMP sweep, are considered in this study. In SIMPrestart, multiple trials of SIMP are run with each trial using a different volume fraction constraint,  $\hat{V}_f$ . For each of these trials, SIMP was initialised from a random solution normalised to

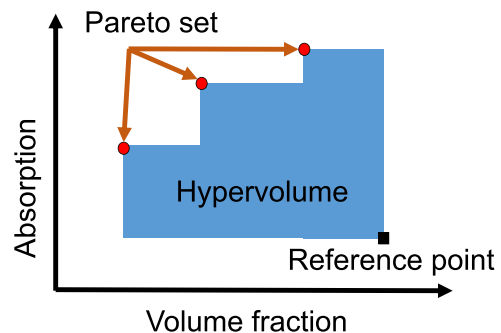


FIG. 2. (Color online) An illustration of the hypervolume metric.

have an overall initial volume fraction close to the chosen  $\hat{V}_f$ . Once convergence is achieved, SIMP is restarted with a new  $\hat{V}_f$  and a newly generated initial solution. SIMPsweep starts from an empty or air-filled solution with an initial volume fraction limit of  $\hat{V}_f = 0$  and applies SIMP move updates while updating  $\hat{V}_f$  in every iteration, reaching  $\hat{V}_f = 1$  as the fitness evaluation budget is reached. The solutions from SIMP algorithms do not always result in discrete zero or one shapes, and the shapes are rounded, i.e., values less than 0.5 are set to zero and values more than 0.5 are set to one, and the absorptions are recomputed. This involved additional fitness evaluations beyond the budget. Nevertheless, the resulting changes in absorption due to rounding are expected to be insignificant.

### B. CHg

CHg starts from an empty or air-filled design domain and fills porous material incrementally in finite elements, where the gradient of sound absorption  $\partial\bar{\alpha}/\partial\chi_i$  is highest. At each step,  $m$  elements are chosen to be filled with porous material after each gradient evaluation, and the total number of fitness evaluations necessary would be  $n_e/m$ , where  $n_e$  is the total number of elements.  $m$  is chosen such that  $n_e/m$  does not exceed the budget. Note that CHg searches solutions in the discrete space because an element is either filled or not filled, unlike that in the SIMP algorithms.

Note that it is possible to speed up gradient algorithms if required. For example, if the allocated fitness evaluation budget is reduced by a factor of ten, for SIMPsweep, the volume fraction constraint,  $\hat{V}_f$ , can be adapted ten times quickly; in CHg, the number of elements filled,  $m$ , can be increased ten times. For SIMPstart, speed-up can be achieved by tuning the move limit parameter,  $m$ , but should be performed with care to avoid numerical oscillations.

## IV. NON-GRADIENT APPROACHES

### A. Hill climbing

Hill climbing is a single-objective optimisation technique wherein an initial solution is picked and iteratively modified, and the modified solution is accepted as the current solution if it is improving. To adapt this method for multi-objective optimisation, the two objectives  $\bar{\alpha}$  and  $V_f$  are combined into a scalar value using

$$\min_{\mathbf{x}} C = -w\bar{\alpha} + (1 - w)V_f. \tag{4}$$

The weight,  $w$ , corresponds to the importance of maximising absorption as opposed to minimising volume fraction and can take values between zero and one. A weight of one implies maximising only absorption irrespective of volume fraction and, likewise, a weight of zero corresponds to only minimising volume fraction. An illustration of the effect of choosing  $w$  on the scalarised objective is shown in Fig. 3. Note that  $w$  governs the slope of the isolines of the scalarised objective. This will be relevant in hybrid algorithm 1. For each trial run of HC, a fixed weight is chosen. Then, hill climbing on the combined objective is performed until the fitness evaluation budget is used up. Fifteen such trials are run with different weights.

### B. NSGA-II

NSGA-II is a popular multi-objective optimisation strategy introduced by Deb *et al.*<sup>29</sup> It has been effectively used in solving multi-criteria decision-making problems across a plethora of fields. In this implementation of NSGA-II, a single-point crossover with an individual crossover probability of 0.9 is applied with a bit-wise mutation rate of  $(1/n_e)$ , where  $n_e$  is the chromosome length, and a population size of 32. These parameters were chosen based on parameter-tuning studies on genetic algorithms.<sup>9</sup>

### C. Random search algorithm (RAND)

For benchmarking the performance of HC and NSGA-II, a RAND is also applied on all of the seven problem instances. For this, random solutions spread across volume fraction are obtained by choosing a random number for desired volume fraction and using this value as probability to fill porous material in each element.

## V. HYBRID APPROACHES

From the studies on gradient and non-gradient algorithms, it was observed that gradient methods can quickly approximate the Pareto front, whereas non-gradient methods can provide improvements in specific regions of the Pareto front. To obtain the benefits of both, two hybrid approaches, combining a gradient-based algorithm for initiation and a non-gradient algorithm for improvement, are presented and compared. The first hybrid approach is a combination of CHg and HC, denoted as HA1, and the second hybrid approach is a combination of CHg and NSGA-II, denoted as HA2. CHg was picked as the initiator mainly because it

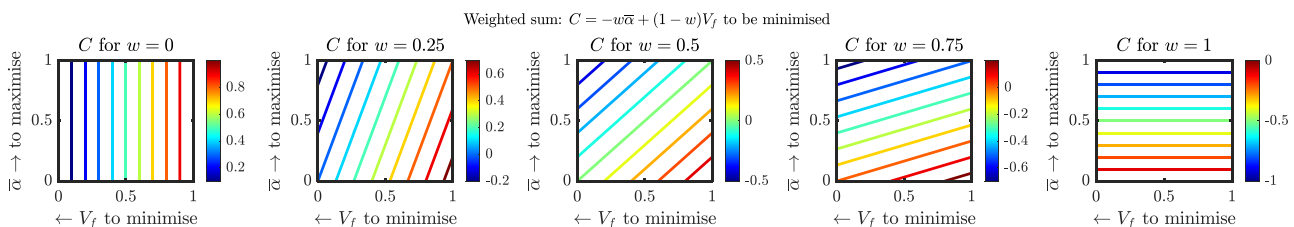


FIG. 3. (Color online) The effect of weights in weighted-sum scalarisation on the isolines of combined objective value. Note that  $w$  governs the slope of the isolines.

guarantees discrete solutions and allows the possibility to speed up.

**A. Hybrid approach 1: CHg + HC**

HA1 combines the use of CHg for 25% of the budget and HC for the remaining 75% of the budget. These numbers are arbitrarily chosen with some basis on experience. Because CHg is gradient-based, and gradient-included evaluations are thrice as expensive as non-gradient fitness evaluations [Eq. (3)], the rationing is such that CHg uses  $25\% \times (4096/3)$  fitness evaluations and HC uses  $75\% \times (4096/1)$  fitness evaluations.

Figure 4 illustrates the procedure involved in HA1. First, CHg is run to obtain a trade-off solution set. Then, 15 solutions are selected from the CHg trade-off set equispaced in volume fraction to use as initial solutions for each of the 15 HC trials. For each HC trial, a different scalarisation weight,  $w$ , is used such that the isolines of the combined objective,  $C$ , have a slope tangential to CHg Pareto front at the initial solution. The slope of the Pareto front at the initial solution is obtained using a simple central difference of adjacent points. This ‘‘Pareto-slope-based scalarisation’’ effectively guides HC to find improvements to the Pareto front. HC is run until the remaining budget is used up. Figure 4 shows the progress of solutions in the objective space in an arbitrarily chosen trial of HA1. The CHg Pareto front is depicted in magenta dashed lines. A solution marked in blue circle is picked and based on the Pareto-slope at this point marked in solid black line, and hill climbing is applied with a scalarisation weight,  $w$ , chosen such that the scalarised isolines (see Fig. 3) match the Pareto tangent. It may be observed that new improving solutions better in frequency-averaged

absorption and volume fraction are found by the HC improver. Also, only a specific region is explored. The combined Pareto front from all of the 15 trials of HA1 is marked in red crosses.

**B. Hybrid approach 2: CHg + NSGA-II**

HA2 combines CHg and NSGA-II in a similar fashion, i.e., CHg uses 25% of the budget, and NSGA-II uses the remaining 75% of the budget. The rationing of fitness evaluations is similar to that in HA1. When there were more solutions in CHg Pareto set, only 32 solutions equispaced in volume fraction were considered as the initial population for NSGA-II, and when there were less solutions, they were duplicated using the selection process in the first generation. Then, NSGA-II is run for the remainder of the budget.

Figure 5 shows the solutions searched in an example trial out of the 15 trials that were run for problem instance 1. After obtaining the CHg Pareto front displayed in magenta, 32 equispaced points were picked as the initial population for NSGA-II, resulting in the blue points. The overall Pareto front shown in red crosses includes some better solutions (beyond  $V_f = 0.2$ ), which dominate the CHg Pareto front in terms of  $\bar{\alpha}$  and  $V_f$ .

**C. Overall comparison**

**1. Trial-averaged performance**

Table IV shows an overall comparison of the resulting hypervolumes covered by all of the algorithms for all of the problem instances. These hypervolumes were obtained by allowing 1365 fitness evaluations for gradient algorithms and 4096 gradient-free fitness evaluations for non-gradient algorithms. These fitness evaluations correspond to giving the same computational time for all of the algorithms.

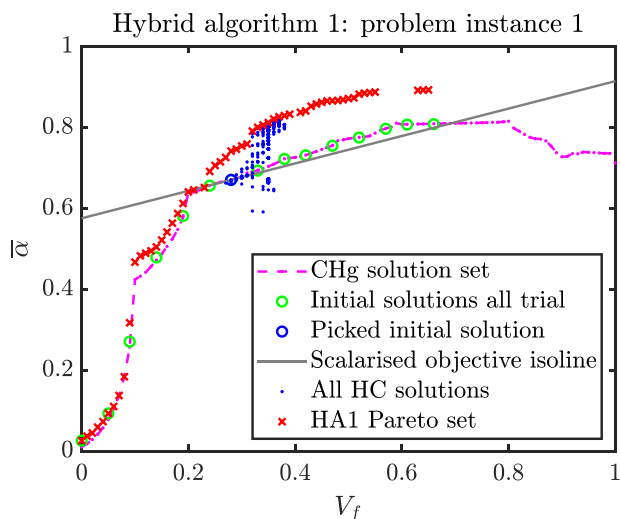


FIG. 4. (Color online) The HA1 illustration of a trial for problem instance 1, which consists of applying CHg for 25% of the budget, picking an initial solution on the CHg Pareto set, setting scalarisation weight such that the isolines of the combined objective are tangential to the Pareto front at the selected CHg point, and applying hill climbing for the rest of the fitness evaluation budget. The final Pareto set after combining 15 trials, with each starting from equispaced points on the CHg Pareto set, are shown using ‘‘x’’ markers.

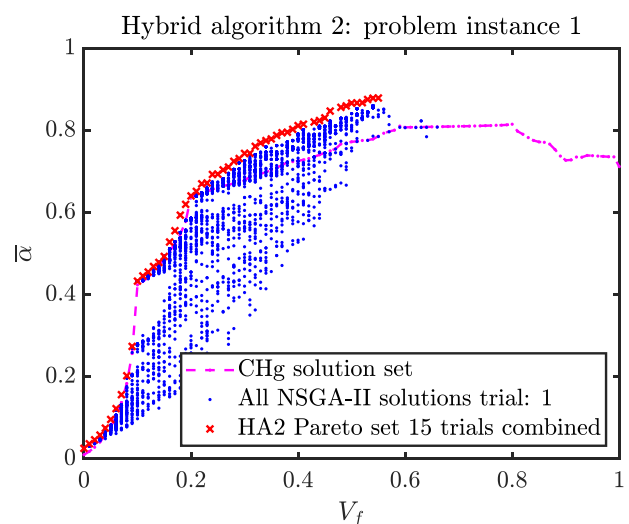


FIG. 5. (Color online) The HA2, where CHg is run for 25% of computational budget, then using the Pareto set as the initial population, and NSGA-II is run for the remaining budget. Solutions traversed by NSGA-II in 1 of the 15 trials are shown with blue dots. The combined Pareto front from 15 trials is shown with red crosses.

TABLE IV. Median hypervolumes obtained while running one trial with a budget equivalent to 4096 gradient-free fitness evaluations. Best values are highlighted in bold for each problem instance. HA2 seems to perform best when considering the trial-averaged performance for 4096 fitness evaluations.

Fitness evaluations Instance/algorithm	Gradient-based			Gradient-free			Hybrid	
	1365 SIMPrestart	1365 SIMPswEEP	$\min(n_e/m, 1365)$ CHg	4096 HC	4096 NSGA-II	4096 RAND	4096 HA1	4096 HA2
1	0.71	0.68	0.67	0.56	0.68	0.59	0.70	<b>0.72</b>
2	0.40	0.40	<b>0.41</b>	0.27	0.34	0.32	<b>0.41</b>	<b>0.41</b>
3	0.73	0.61	<b>0.74</b>	0.59	0.63	0.61	0.73	0.72
4	<b>0.12</b>	<b>0.12</b>	0.11	0.09	0.11	0.11	0.11	<b>0.12</b>
5	0.52	<b>0.53</b>	<b>0.53</b>	0.38	0.48	0.46	<b>0.53</b>	<b>0.53</b>
6	0.72	<b>0.76</b>	0.75	0.54	0.66	0.62	<b>0.76</b>	<b>0.76</b>
7	0.87	0.86	0.87	0.71	0.85	0.77	0.87	<b>0.88</b>

Because 15 trials were run for non-gradient and hybrid algorithms, the median-trial hypervolume is shown. The highest hypervolumes rounded to two decimal places are shown in bold font, indicating that the algorithm performs best on that problem instance.

Among the gradient methods, it is worth noting that SIMPswEEP performs the best in more problem instances than SIMPrestart, whereas the SIMPswEEP and CHg are similar, performing best in three problem instances each. Notably, SIMPswEEP and CHg are also scalable for lower budgets.

Between HC and NSGA-II, NSGA-II consistently spans a higher hypervolume across all of the problem instances. This is because based on the choice of scalarisation weight, in a given trial, HC only explores a specific region in the Pareto front. NSGA-II spans the objective space effectively because of the crowding-distance-based selection mechanism. NSGA-II also outperforms RAND in all of the problem instances, but, interestingly, HC on a per-trial basis, does not outperform even RAND. This is because HC in a single trial is essentially a single-objective algorithm that does not incentivise spanning the hypervolume. Neither HC nor NSGA-II resulted in best hypervolumes in any of the problem instances, highlighting the deficiency of non-gradient methods in multi-objective topology optimisation.

Overall, the hybrid algorithms result in a better hypervolume in more problem instances than the parent gradient or non-gradient methods. Note that HA2 performs better than stand-alone NSGA-II for the same budget. While it is evident that gradient-based initialisation boosts the performance of NSGA-II, it is interesting to note that HA2 can perform better than SIMPrestart or SIMPswEEP, which are normally used in practise. Thus, if one has a fixed computational budget to cover the most hypervolume, it may be worth exploring the use of CHg followed by NSGA-II.

## 2. Combined performance across 15 trials

It is also of interest to identify effective strategies that find solutions with best attainable quality with longer computational time budgets, such as for manufacturing best acoustic designs. Table V shows the resulting hypervolumes covered by a combination of 15 trials, which is equivalent to  $15 \times 4096$  gradient-free function evaluations. For this

comparison, gradient methods are not included as they do not use the same budget.

In this comparison, HC shows a significant improvement as it is able to combine the good solutions from various regions of the Pareto front. For the same reason, HA1, which is a combination of CHg and HC, also performs exceptionally well and produces the best hypervolumes in all of the problem instances. This shows that the proposed Pareto-slope-based weighted-sum scalarisation technique with a simple greedy hill climbing algorithm can be used as an effective local improvement strategy. A take-away is that before manufacturing an optimal shape using any multi-objective topology optimisation approach, it is worth ensuring that there exists no other dominating solution that HC can find.

Between NSGA-II and its hybrid counterpart, HA2, the latter seems to cover more hypervolumes across all of the problem instances. This is another example of a hybrid approach performing better than its parent approach. HA2 also performs among the best in three problem instances and comes close to the performance of HA1. This shows that there is benefit to using hybrid strategies involving gradient initialisers with non-gradient improvers.

## 3. Manufacturability considerations

While the hybrid algorithms are able to span better hypervolumes, a natural question that arises is whether these acoustic material shapes are feasible to be manufactured.

TABLE V. Here, hypervolumes combined over 15 trials are compared. These hypervolumes are also contrasted with those of single trials of gradient algorithms. Best values are highlighted in bold for each problem instance.

Instance Budget	Gradient-free			Hybrid	
	HC $15 \times 4096$	NSGA-II $15 \times 4096$	RAND $15 \times 4096$	HA1 $15 \times 4096$	HA2 $15 \times 4096$
1	<b>0.74</b>	0.73	0.62	<b>0.74</b>	0.73
2	0.40	0.36	0.33	<b>0.41</b>	0.40
3	0.78	0.69	0.62	<b>0.81</b>	0.73
4	0.11	<b>0.12</b>	0.11	<b>0.12</b>	<b>0.12</b>
5	0.52	0.50	0.47	<b>0.53</b>	<b>0.53</b>
6	0.75	0.63	0.63	<b>0.77</b>	0.76
7	0.84	0.87	0.80	<b>0.88</b>	<b>0.88</b>



Figure 6 shows the Pareto solutions in the absorption vs volume fraction space with a few optimal shapes for each algorithm for problem instance 6.

The optimal acoustic shapes from SIMPstart exhibit a wide range of features, from circular cavities to flat-layered structures to complex and intricate patterns. These features seem to be dependent on the random initial solution picked. For this problem instance, the general trend is that as more porous materials are added in the design domain, the frequency-averaged absorption also increases. For SIMPsweep,

the optimal shapes closely resemble a single flat layer of porous material at low volume fraction for this melamine problem instance. However, when considering other problem instances, patterns other than flat-layered shapes were also produced. It should be noted that these shapes are rounded to remove any intermediate material elements that were present. For CHg, the shapes have two flat layers as opposed to one, as found in SIMPsweep.

In general, the gradient algorithms produced meaningful shapes, whereas non-gradient algorithms produced

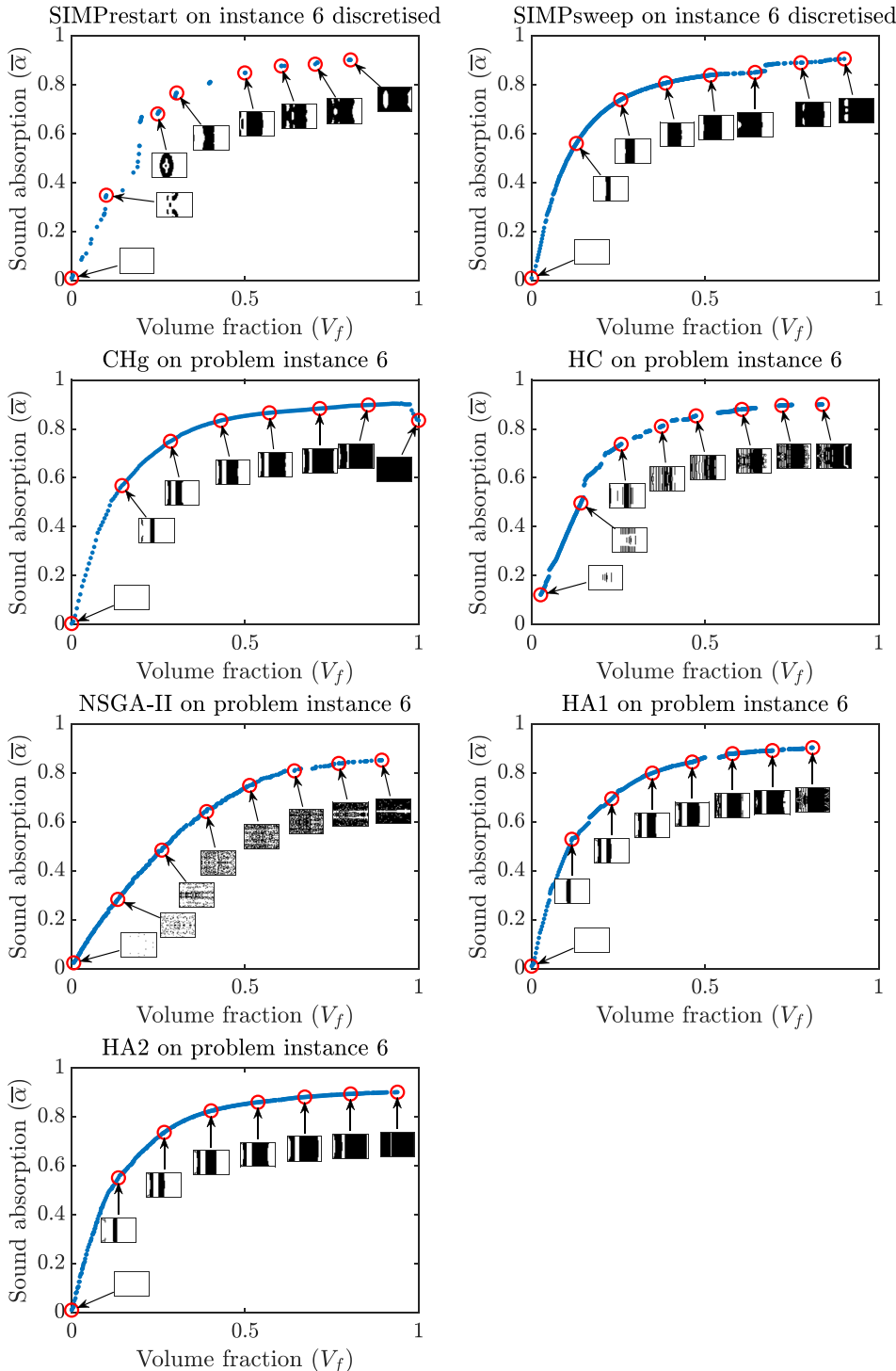


FIG. 6. (Color online) Pareto optimal shapes produced by all of the algorithms for the same computational budget for problem instance 6.

indeterminate shapes. The shapes produced by HC resembled alternating layers of porous material and air, and NSGA-II did not converge to meaningful shapes on this problem instance for the budget considered. In cases where gradient formulations are not available, appropriate filtering techniques are suggested to produce meaningful shape patterns.

Among the hybrid algorithms, the shapes from HA1 and HA2 resembled two flat layers of porous material separated by an air layer likely due to the initialisation with CHg. Some differences can be observed at higher volume fractions, where HA1 produced intricate shapes while HA2 retained the two distinct layered shapes.

Figure 7 shows a few trade-off shapes and their absorption curves for HA2 and compares them with SIMPstart for problem instance 6. Near a volume fraction of 0.25, while SIMPstart finds a shape with a blob of porous material with a cavity, HA2 is able to find a slightly better absorbing solution with two thin flat layers. SIMPstart is unable to converge to this shape because it reaches a local optimum. While observing the differences in absorption curves, it is seen that the peak absorption occurs at slightly different frequencies. At a volume fraction of 0.5, the absorption curves are similar even though the shapes are considerably different. At higher volume fractions, SIMPstart finds a solution with a thick porous layer with an enclosed air cavity, whereas the HA2 solution retains the double-flat-layered shape. While the SIMPstart shape has a slightly lower absorption around 1000 Hz with a lower frequency cutoff, the double-flat-layered-shape exhibits consistently high absorption after a slightly higher cutoff frequency. These two shapes do not differ significantly in frequency-averaged sound absorption.

#### 4. Discussions and perspectives

In general, certain shape features seem to be preferred in the acoustic shape designs across problem instances such as the presence of an air backing in front of the rigid wall.

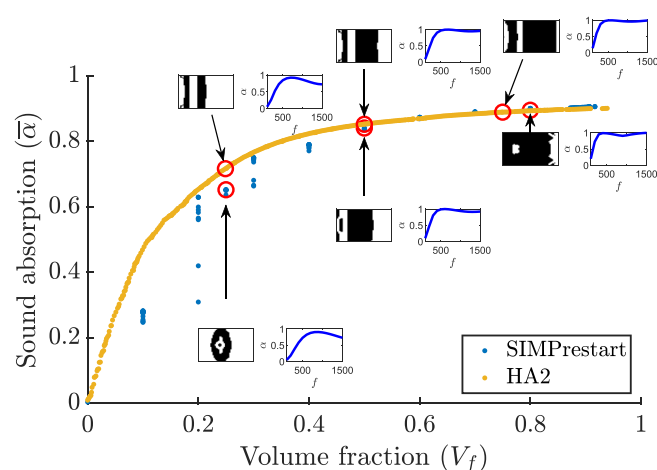


FIG. 7. (Color online) Comparison of Pareto shapes and their absorption vs frequency curves from SIMPstart and HA2 algorithms for problem instance 6. The absorption curves are plotted beside the shapes.

For melamine problem instances, flat-layered shapes were optimal on many occasions, but it was also common to observe inverted wedge-shaped designs resembling a reversed anechoic chamber wedge. Intricate shapes with two-dimensional features occurred occasionally and were predominantly the case for poroelastics with high airflow resistivity. With regard to the algorithm choice, if acoustic designers are interested in quickly obtaining shape designs for conceptual design, gradient methods, such as SIMPsweep or CHg, are recommended. If the goal is to fabricate and install optimised shapes in practical applications, hybrid algorithms are recommended to ensure that suboptimal designs are not chosen.

While in many instances, the variation of materials in optimal shapes is in the primary direction of wave propagation, in some cases, the optimal shapes have two-dimensional material distribution, justifying the need for topology optimisation. A three-dimensional (3D) topology optimisation setup could enable more intricate propagation paths and, hence, potentially better absorbing solutions.

In the current study, efficient optimisation strategies have been explored by comparing methods likely to be used by other researchers. An extension to this study may be to investigate other topology optimisation paradigms such as moving morphable components and level-set. Methods like ESO/BESO use a term such as stress to modify the shape for compliance minimisation. It would be of interest to explore the existence of a field variable analogous to stress in acoustic applications. Such studies could pave the way for *informed* heuristics and use domain-specific knowledge that could prove more efficient. Additionally, the current computational bottleneck is solving the finite element system. An area of interest is to explore incremental evaluation strategies that allow quick solution computation for slightly modified shapes.

#### VI. CONCLUSION

In this article, several multi-objective topology optimisation strategies were compared with the goal of identifying effective approaches for obtaining lightweight and high-absorbing acoustic shape designs within a given amount of computational effort. Several commonly used optimisation strategies, including SIMP, NSGA-II, weighted-sum hill climbing, and constructive heuristics, were tested across seven benchmark problems involving a simple impedance tube system. The results showed that gradient algorithms could quickly converge to good-quality solutions but occasionally get stuck at local-optimal shapes. This is indicated by the fact that non-gradient approaches have been able to find better solutions in terms of absorption and volume fraction objectives. Hence, we tested hybrid algorithms that use gradient algorithms as initialisers and non-gradient algorithms for local improvement. The results reveal that for the same computational budget, hybrid algorithms can consistently find better acoustic shapes than their parent gradient or non-gradient methods. We also introduced a novel

Pareto-slope-based hill climbing that could be used for effective local improvement. Such techniques may benefit acoustic engineers by revealing the existence of lightweight and better absorbing solutions, thereby avoiding choosing suboptimal shapes for additive manufacturing.

## ACKNOWLEDGMENTS

This result is part of a project that received funding from the European Research Council (ERC) under the Horizon 2020 Research and Innovation Programme, No2Noise<sup>1</sup> with Grant Agreement No. 765472.

<sup>1</sup>See no2noise.eu (Last viewed May 9, 2023).

- <sup>1</sup>T. Cambonie, F. Mbailassem, and E. Gourdon, "Bending a quarter wavelength resonator: Curvature effects on sound absorption properties," *Appl. Acoust.* **131**, 87–102 (2018).
- <sup>2</sup>J. S. Lee, Y. Y. Kim, J. S. Kim, and Y. J. Kang, "Two-dimensional poroelastic acoustical foam shape design for absorption coefficient maximization by topology optimization method," *J. Acoust. Soc. Am.* **123**(4), 2094–2106 (2008).
- <sup>3</sup>W. U. Yoon, J. H. Park, J. S. Lee, and Y. Y. Kim, "Topology optimization design for total sound absorption in porous media," *Comput. Methods Appl. Mech. Eng.* **360**, 112723 (2020).
- <sup>4</sup>O. Sigmund and K. Maute, "Topology optimization approaches," *Struct. Multidiscip. Optim.* **48**(6), 1031–1055 (2013).
- <sup>5</sup>M. P. Bendsøe and N. Kikuchi, "Generating optimal topologies in structural design using a homogenization method," *Comput. Methods Appl. Mech. Eng.* **71**(2), 197–224 (1988).
- <sup>6</sup>M. P. Bendsøe, "Optimal shape design as a material distribution problem," *Struct. Optim.* **1**(4), 193–202 (1989).
- <sup>7</sup>E. Wadbro and M. Berggren, "Topology optimization of an acoustic horn," *Comput. Methods Appl. Mech. Eng.* **196**(1-3), 420–436 (2006).
- <sup>8</sup>M. B. Dühring, J. S. Jensen, and O. Sigmund, "Acoustic design by topology optimization," *J. Sound Vib.* **317**(3-5), 557–575 (2008).
- <sup>9</sup>V. T. Ramamoorthy, E. Özcan, A. J. Parkes, A. Sreekumar, L. Jaouen, and F.-X. Bécot, "Comparison of gradient-based and gradient-free heuristics and metaheuristics for topology optimisation in acoustic porous materials," *J. Acoust. Soc. Am.* **150**(4), 3164–3176 (2021).
- <sup>10</sup>J. W. Lee and Y. Y. Kim, "Topology optimization of muffler internal partitions for improving acoustical attenuation performance," *Int. J. Numer. Methods Eng.* **80**(4), 455–477 (2009).
- <sup>11</sup>G. H. Yoon, "Acoustic topology optimization of fibrous material with Delany–Bazley empirical material formulation," *J. Sound Vib.* **332**(5), 1172–1187 (2013).
- <sup>12</sup>J. S. Lee, P. Göransson, and Y. Y. Kim, "Topology optimization for three-phase materials distribution in a dissipative expansion chamber by unified multiphase modeling approach," *Comput. Methods Appl. Mech. Eng.* **287**, 191–211 (2015).
- <sup>13</sup>E. L. Yedeg, E. Wadbro, and M. Berggren, "Interior layout topology optimization of a reactive muffler," *Struct. Multidiscip. Optim.* **53**(4), 645–656 (2016).
- <sup>14</sup>J. Kook, K. Koo, J. Hyun, J. S. Jensen, and S. Wang, "Acoustical topology optimization for Zwicker's loudness model—Application to noise barriers," *Comput. Methods Appl. Mech. Eng.* **237-240**, 130–151 (2012).
- <sup>15</sup>K. H. Kim and G. H. Yoon, "Optimal rigid and porous material distributions for noise barrier by acoustic topology optimization," *J. Sound Vib.* **339**, 123–142 (2015).
- <sup>16</sup>L. Chen, C. Liu, W. Zhao, and L. Liu, "An isogeometric approach of two dimensional acoustic design sensitivity analysis and topology optimization analysis for absorbing material distribution," *Comput. Methods Appl. Mech. Eng.* **336**, 507–532 (2018).
- <sup>17</sup>Z.-x. Xu, H. Gao, Y.-j. Ding, J. Yang, B. Liang, and J.-c. Cheng, "Topology-optimized omnidirectional broadband acoustic ventilation barrier," *Phys. Rev. Appl.* **14**(5), 054016 (2020).
- <sup>18</sup>Y. Xu, W. Zhao, L. Chen, and H. Chen, "Distribution optimization for acoustic design of porous layer by the boundary element method," *Acoust. Aust.* **48**, 107–119 (2020).
- <sup>19</sup>H. A. Eschenauer and N. Olhoff, "Topology optimization of continuum structures: A review," *Appl. Mech. Rev.* **54**(4), 331–390 (2001).
- <sup>20</sup>G. I. N. Rozvany and T. Lewiński, *Topology Optimization in Structural and Continuum Mechanics* (Springer, New York, 2014).
- <sup>21</sup>J. Liu, A. T. Gaynor, S. Chen, Z. Kang, K. Suresh, A. Takezawa, L. Li, J. Kato, J. Tang, C. C. Wang, L. Cheng, X. Liang, and A. C. To, "Current and future trends in topology optimization for additive manufacturing," *Struct. Multidiscip. Optim.* **57**(6), 2457–2483 (2018).
- <sup>22</sup>O. Sigmund, "A 99 line topology optimization code written in MATLAB," *Struct. Multidiscip. Optim.* **21**(2), 120–127 (2001).
- <sup>23</sup>K. Suresh, "A 199-line MATLAB code for Pareto-optimal tracing in topology optimization," *Struct. Multidiscip. Optim.* **42**(5), 665–679 (2010).
- <sup>24</sup>A. M. Mirzendehtel and K. Suresh, "A Pareto-optimal approach to multi-material topology optimization," *J. Mech. Des.* **137**(10), 101701 (2015).
- <sup>25</sup>Y.-F. Fu, "Recent advances and future trends in exploring Pareto-optimal topologies and additive manufacturing oriented topology optimization," *Math. Biosci. Eng.* **17**(5), 4631–4656 (2020).
- <sup>26</sup>Y. M. Xie and G. P. Steven, "A simple evolutionary procedure for structural optimization," *Comput. Struct.* **49**(5), 885–896 (1993).
- <sup>27</sup>Y. M. Xie and G. P. Steven, "Evolutionary structural optimization for dynamic problems," *Comput. Struct.* **58**(6), 1067–1073 (1996).
- <sup>28</sup>R. Kasimbeyli, Z. K. Ozturk, N. Kasimbeyli, G. D. Yalcin, and B. I. Erdem, "Comparison of some scalarization methods in multiobjective optimization," *Bull. Malays. Math. Sci. Soc.* **42**(5), 1875–1905 (2019).
- <sup>29</sup>K. Deb, S. Agrawal, A. Pratap, and T. Meyarivan, "A fast elitist non-dominated sorting genetic algorithm for multi-objective optimization: NSGA-II," in *International Conference on Parallel Problem Solving from Nature* (Springer, New York, 2000), pp. 849–858.
- <sup>30</sup>S. Verma, M. Pant, and V. Snasel, "A comprehensive review on NSGA-II for multi-objective combinatorial optimization problems," *IEEE Access* **9**, 57757–57791 (2021).
- <sup>31</sup>W. Liu, H. Zhu, Y. Wang, S. Zhou, Y. Bai, and C. Zhao, "Topology optimization of support structure of telescope skin based on bit-matrix representation NSGA-II," *Chin. J. Aeronaut.* **26**(6), 1422–1429 (2013).
- <sup>32</sup>X. Guo, W. Zhang, and W. Zhong, "Doing topology optimization explicitly and geometrically—A new moving morphable components based framework," *J. Appl. Mech.* **81**(8), 081009 (2014).
- <sup>33</sup>G. Allaire, F. Jouve, and A.-M. Toader, "A level-set method for shape optimization," *C. R. Math.* **334**(12), 1125–1130 (2002).
- <sup>34</sup>M. Y. Wang, X. Wang, and D. Guo, "A level set method for structural topology optimization," *Comput. Methods Appl. Mech. Eng.* **192**(1-2), 227–246 (2003).
- <sup>35</sup>N. Atalla, R. Panneton, and P. Debergue, "A mixed displacement-pressure formulation for poroelastic materials," *J. Acoust. Soc. Am.* **104**(3), 1444–1452 (1998).
- <sup>36</sup>D. L. Johnson, J. Koplik, and R. Dashen, "Theory of dynamic permeability and tortuosity in fluid-saturated porous media," *J. Fluid Mech.* **176**, 379–402 (1987).
- <sup>37</sup>Y. Champoux and J.-F. Allard, "Dynamic tortuosity and bulk modulus in air-saturated porous media," *J. Appl. Phys.* **70**(4), 1975–1979 (1991).
- <sup>38</sup>D. Lafarge, P. Lemarinier, J. F. Allard, and V. Tarnow, "Dynamic compressibility of air in porous structures at audible frequencies," *J. Acoust. Soc. Am.* **102**(4), 1995–2006 (1997).
- <sup>39</sup>E. Andreassen, A. Clausen, M. Schevenels, B. S. Lazarov, and O. Sigmund, "Efficient topology optimization in MATLAB using 88 lines of code," *Struct. Multidiscip. Optim.* **43**(1), 1–16 (2011).